

Mechanical Properties of Friction Stir Butt-Weld 6061-T6 Aluminum Alloy Using Taguchi-Based GRA

BEERE HARI KUMAR¹, N. PHANI RAJA RAO², T SURYA SEKHARA REDDY³

¹PG student, Dept. of Mechanical Engineering, SVIT, Anantapur.

²Assistant Professor & Head of the department, Dept. of Mechanical Engineering, SVIT, Anantapur.

³Principal & Professor, Dept. of Mechanical Engineering, SVIT, Anantapur.

ABSTRACT

The use of aluminum alloys, nowadays, is swiftly growing from the prerequisite of producing higher strength to weight ratio. Lightweight components are crucial interest in most manufacturing sectors, especially in transportation, aviation, maritime, automotive, and others. Traditional available joining methods have an adverse effect on joining these lightweight engineering materials, increasing needs for new environmentally friendly joining methods. Hence, friction stir welding (FSW) is introduced. Friction stir welding is a relatively new welding process that can produce high-quality weld joints with a lightweight and low joining cost with no waste. This paper endeavors to deal with optimizing process parameters for quality criteria on tensile and hardness strengths. Samples were taken from a 5 mm 6061-T6 aluminum alloy sheet with butt joint configuration. Controlled process parameters tool profile, rotational speed and transverse speed were utilized. The process parameters are optimized making use of the combination of Grey relation analysis method and L_9 orthogonal array. Mechanical properties of the weld joints are examined through tensile, hardness, and liquid penetrant tests at room temperature. From this research, rotational speed and traverse speed become significant parameters at a 99% confidence interval, and the joint efficiency reached 91.3%.

Keywords: friction stir welding, AA6061, grey relation, orthogonal array

1. INTRODUCTION

FSW is a new class of joining technique being employed for a broad kind of similar and dissimilar metals and alloys. It is an approach of fabrication (i.e., solid state thermo-mechanical), where the temperature of welding comparatively below the

base metal melting point [8, 3, 14]. In the process of FSW, friction heat will be produced by a non-expendable rotating tool (comprising of a pin, and shoulder) that is engrossed into the edge of butting. This frictional heat produced at the interface of work piece and tool topically softens the work piece and appropriates the tool to move with a forward motion of the joint. Rotation and translation of tool induce the material flow of work piece from front to back of the pin, which results in welded joint [11]. The hardening of the weld cracking issue does not originate in FSW process due to that the generated heat does not accomplish its melting point. In the same manner, procedure of solid-state welding surmounts other kind of problems in unified aluminum alloys welding like sequestration, porosity, formation of un annealed inter-metallic, and cracking of heat affected area liquation [10], which made the process of FSW as an efficacious approach of welding for grouping a broad kind of metals and alloys those are similar and dissimilar in various field of applications such as automobile, aerospace, and industrial. Recent years, the potentiality of making effective welded joints with alloys or metals which are not similar has acquired a panoptic interest in the field of research because of possible significance in engineering and issues related with traditional welding procedures. However, the control variation of FSW process parameters has substantial impact on the quality of welded joint. It is quite difficult to the process engineer to control these process parameters of FSW due to the conflict nature of these input process parameters with the characteristics of welding quality. In addition, it is also significant to choose these control variables in FSW process for each new component of welding to incur an effectual welded joint as per the specifications of design. Since the components of frictional stir welded dissimilar aluminum alloys find a wide variety of applications in aircraft, automotive and industrial structures whereby possible multi-material configurations involve among others the alloys [1].



Figure: Cause and effect diagram of parameters influencing on FSW joint quality.

2. MATERIALS AND METHODS

This section describes the methods and materials used to perform the experimental investigation of FSW process. The material used in this study was 6061-T6 aluminum alloy with a butt joint configuration. The chemical, mechanical, and thermo-physical properties of this material are depicted in Tables, respectively. The welding sheet was cut off parallel into the rolling direction with a dimension of 101.6 mm × 20 mm × 5 mm using a hand hacksaw to minimize the residual stresses that will occur during the cutting operations. In addition, the tensile strength test samples were prepared according to ASTM E8-04 standards as shown in below Figure by making use of a metal craft VMBS 1610 band saw machine.

Table: Chemical composition of AA 6061 material.

Material %	Mg	Si	Fe	Cr	Cu	AL
AA 6061	0.92	0.6	0.33	0.18	0.25	97.72

Table: Mechanical property of AA 6061 material.

Material	Yield Strength (MPa)	Ultimate Tensile Strength (MPa)	Hardness (HRA)
AA6061	276	310	40

Table: Thermo-physical properties of 6061 aluminum alloy material.

3. SYSTEM DESIGN

Density (g/cm ³)	Melting Point (°C)	Thermal Conductivity (W/m-k)	Specific Heat (J/Kg-°C)
2.7	652	167	0.896

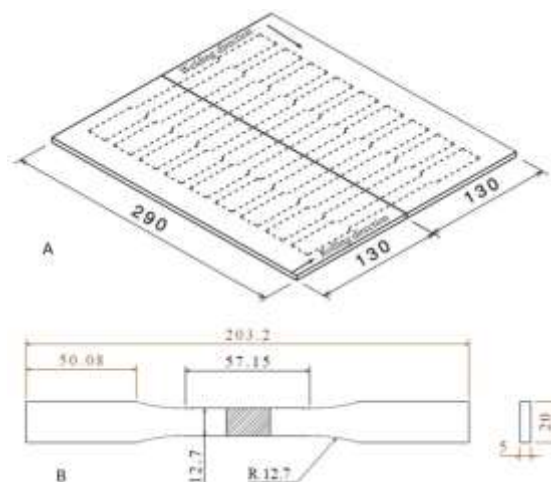


Figure 2. Pattern of welding with respect to rolling direction and removal of tensile specimen:

(A) Dimension of the flat tensile specimen, (B) welded specimen according to (ASTM E8-04).

3. EXPERIMENTAL SETUP

The experimental setup depicted in Figure 3 was carried out on a high-precision XHS7145 vertical CNC machine (Shanghai Bairuo Testing Instrument Co., Ltd., Shanghai, China) with a maximum speed of 8000 rpm. The welding tool was used for the experimentation made from H13 tool steel with different pin profiles. The mechanical property and chemical composition of H13 tool are listed respectively in Tables 4 and 5. The tool pin length geometrical dimension, represented in Figure 4, was prepared at 0.3 mm less than the base metal thickness for minimizing the tool wear during the welding. The tensile strengths of the weld joint samples are depicted in Figure 5 and were measured by the Bairuo computer controlled electro-hydraulic universal testing machine (Shandong Lunan machine Tool (Group) Co.,Ltd., Shandong, China) of model HUT-600. Besides, the hardness of the joint was measured by the Rockwell hardness-testing machine in scale A. The transient heating that occurs during the welding process was measured by K type thermocouples at a center symmetry point on the advancing and retreating side of the specimen. Digital data logger with the integration of compression type load-cell and data transmitter controlled the axial force of the tool. The parameters identified for this study are tool rotation speed, traverse speed, and tool pin profile. The selected process parameters and their levels are shown in Table 6. Moreover, the quality of FSW was governed by utilizing a firmly secured fixture.

Hence, the work piece fixture was designed to avoid any unwanted free vibrations.



Figure: Experimental setup used for FSW connected with the load cell and thermocouples

Table: Mechanical properties of H13 tool steel.

Material	%C	%Si	%Cr	%Mo	%V
H13	0.4	1.00	5.30	1.4	1.0

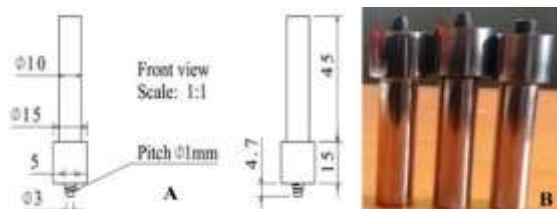


Figure: (A) Geometric dimensions of the tool, (B) From left to right tri-flute threaded, taper threaded and cylindrical threaded tools.



Figure: Extraction of tensile specimens: (A) Welded specimens before the tensile test (B) welded specimens after the tensile test.

Table : Control process parameters and their levels

4. TESTING

a) Tensile Strength

Tensile strength is one of the responses that was measured triple times at room temperatures for similar FS welded of Al-alloys (6061). The effect of rotational speed on the tensile strength has been shown in Figure 6 and the highest tensile strength of 283 MPa was observed from a taper pin profile tool at a rotational speed of 1400 rpm, and traverse speed of 37.5 mm/min and its joint efficiency was reached about 91.3%. Similarly, the lowest tensile strength

of 217 MPa was observed at 900 rpm, traverse speed of 47.5 mm/min, and tri-flute threaded tool pin profile. The result shows that hardness and tensile strength are directly proportional to the rotational speed and inversely proportional to the traverse speed of the tool for this reason: that the lower traverse speed and higher rotational speed produce adequate heat for joining the base metal.

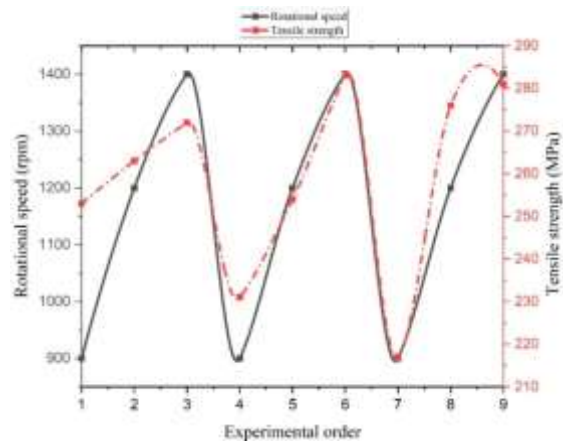


Figure: Effects of rotational speed on the tensile strength property of AA 6061.

b) Hardness

The hardness of the joint was measured three times at the nugget zone. The higher hardness value of 71.6 HR was obtained at the pick point of the curve in Figure 7 at a parameter setting of a rotational speed of 1400 rpm, traverse speed of 37.5 mm/min, and taper threaded tool pin profile. Correspondingly, the minimum hardness value of 54.23 HR was recorded at a rotational speed of 900 rpm, traverse speed of 47.5 mm/min, and tri-flute threaded tool pin profile. The maximum rotational speed with a combination of a taper threaded tool pin imparts the highest hardness strength.

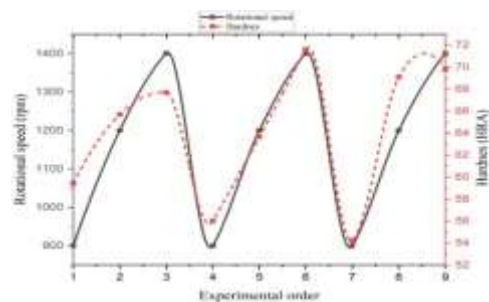


Figure: Effects of rotational speed on the hardness property of AA 6061.

c) Liquid Penetrant Test

As shown in Figure, the test was performed on all 9 experiments along the joint line of the weld. The result shows that Experiment 1, 4, and 8 have a present visible discontinuity along the weld joint. Those experiments, comparatively to the other joints, are more defective. The remaining experiments have a defect-free joint. Surface cracks exist on all of the weld joints at the start and endpoints of the joint. Therefore, the higher rotational speed due to its high heat input and friction delivers defect-free joints. On the other hand, the lower rotational speed has some defects along the welded joints.



Figure: Liquid penetrant test: (A) Welded specimens before the liquid penetrant test; (B) welded specimens after applying penetrants on the faying surfaces; (C) welded specimens after applying developer.

d) Effect of Welding Parameters on the Temperature Profiles

Based on the results of this study, the temperature increased when rotational speed increased due to the severe plastic deformation caused by the high stirring process. At all experiments, the advancing side is affected by a higher temperature than the retreating side shown in Figure. Besides, the temperature is directly proportional to the rotational speed and inversely proportional to the traverse speed.

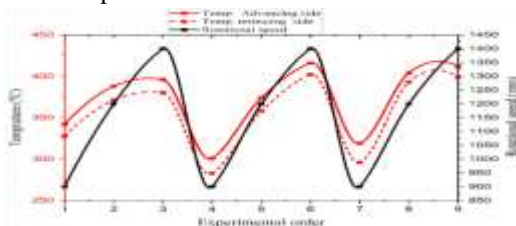


Figure: Correlation between rotational speed and welding temperature.

e) Welding Parameter Effects on the Joint Quality

In the friction stir welding process, a variety of process parameters affects the weld joint quality. FSW welding process parameters mainly include rotational speed of a tool, welding traverse speed and tool profile. Each experimental execution observations have discussed and summarized in.

Experiments 3 and 5 have completely defect-free joints and Experiments 1, 7, and 9 have some flash defects on the advancing sides; but, due to a high RPM and welding speed, they bestow maximum hardness and tensile strength. Therefore, 1200 and 1400 rpm impart defect-free joints for 6061 materials.

CONCLUSION

In this study, a combination of Taguchi based Grey relational analysis method was implemented to come up with the optimal process parameters for FSW. Analyzing the effect of combined factors on the mechanical strengths.

REFERENCES

1. Elnabi, M.M.A.; Osman, T.A.E.; El Mokadem, A.E.; Elshalakany, A.B. Mechanical Properties and Microstructure of Dissimilar Friction Stir Welding of Pure Aluminum to Low Carbon Steel. *Adv. J. Grad. Res.* 2018, 4, 47–58. [CrossRef]
2. Salih, O.S.; Neate, N.; Ou, H.; Sun, W. Influence of process parameters on the microstructural evolution and mechanical characterisations of friction stir welded Al-Mg-Si alloy. *J. Mater. Process. Technol.* 2020, 275, 116366. [CrossRef]
3. Jaiganesh, V.; Sevel, P. Impact of process parameters during friction stir welding of AZ80A Mg alloy. *Sci. Technol. Weld. Join.* 2015, 21, 1–8. [CrossRef]
4. Kundu, J.; Ghangas, G.; Rattan, N.; Kumar, M. Friction Stir Welding: Merits over other Joining Processes. *Int. J. Curr. Eng. Technol.* 2017, 7, 1175–1177.
5. Chaudhary, K. A Review on Advance Welding Processes. *Int. J. Eng. Tech.* 2017, 3, 86–96.

6. Shinde, G.; Gajghate, S.; Dabeer, P.; Seemikeri, C. Low cost friction stir welding: A review. *J. Mater. Today Proc.* 2017, 4, 8901–8910. [CrossRef]
7. Patel, V.; Li, W.; Wang, G.; Wang, F.; Vairis, A.; Niu, P. Friction Stir Welding of Dissimilar Aluminum Alloy Combinations: State-of-the-Art. *J. Met.* 2019, 9, 270. [CrossRef]
8. Shirazi, H.; Kheirandish, S.; Pouraliakbar, H. Employing hooking and effective sheet thickness to achieve optimum failure load in lap joints of friction stir welded AA5456 aluminum. *J. Theor. Appl. Fract. Mech.* 2019. [CrossRef]
9. Fuse, K.; Badheka, V. Bobbin tool friction stir welding: A review. *Sci. Technol. Weld. Join.* 2018. [CrossRef]
10. Magalhães, V.M.; Leitao, C.; Rodrigues, D.M. Friction stir welding industrialisation and research status. *Sci. Technol. Weld. Join.* 2017. [CrossRef]
11. Schubert, E.; Klassen, M.; Zerner, I.; Walz, C.; Sepold, G. Light-weight structures produced by laser beam joining for future applications in automobile and aerospace industry. *J. Mater. Process. Technol.* 2001, 115, 2–8. [CrossRef]
12. Ajri, A.; Rohatgi, N.; Shin, Y.C. Analysis of defect formation mechanisms and their effects on weld strength during friction stir welding of Al 6061-T6 via experiments and finite element modeling. *Int. J. Adv. Manuf. Technol.* 2020, 107, 4621–4635. [CrossRef]
13. Gibson, B.T.; Lammlein, D.; Prater, T.; Longhurst, W.R.; Cox, C.D.; Ballun, M.; Dharmaraj, K.J.; Cook, G.E.; Strauss, A.M. Friction stir welding: Process, automation, and control. *J. Manuf. Process.* 2014, 16, 56–73. [CrossRef]